Article

Pyridinium-Derived *N*-Heterocyclic Carbene Complexes of Platinum: Synthesis, Structure and Ligand Substitution Kinetics

Jonathan S. Owen, Jay A. Labinger, and John E. Bercaw

J. Am. Chem. Soc., **2004**, 126 (26), 8247-8255• DOI: 10.1021/ja040075t • Publication Date (Web): 12 June 2004

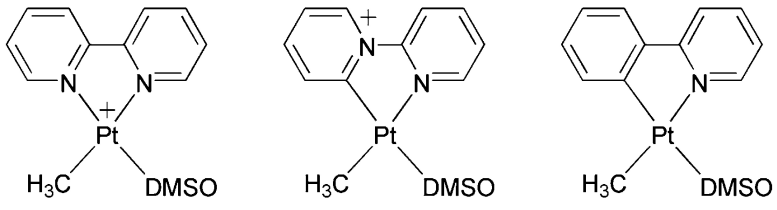

More About This Article

Additional resources and features associated with this article are available within the HTML version:

- Supporting Information
- Links to the 12 articles that cite this article, as of the time of this article download
- Access to high resolution figures
- Links to articles and content related to this article
- Copyright permission to reproduce figures and/or text from this article

View the Full Text HTML

J|A|C|S
ARTICLES
Published on Web 06/12/2004

Pyridinium-Derived *N*-Heterocyclic Carbene Complexes of Platinum: Synthesis, Structure and Ligand Substitution Kinetics

Jonathan S. Owen, Jay A. Labinger,* and John E. Bercaw*

Contribution from the Arnold and Mabel Beckman Laboratories of Chemical Synthesis, California Institute of Technology, Pasadena, California 91125

Received March 5, 2004; E-mail: bercaw@caltech.edu

Abstract: A series of [(R-*iso*-BIPY)Pt(CH_3)L]$^+X^-$ complexes [R-*iso*-BIPY = *N*-(2-pyridyl)-R-pyridine-2-ylidene; (R = 4-H, **1**; 4-*tert*-butyl, **2**; 4-dimethylamino, **3**; 5-dimethylamino, **4**); L = SMe_2, **b**; dimethyl sulfoxide (DMSO), **c**; carbon monoxide (CO), **d**; X = OTf^- = trifluoromethanesulfonate and/or $[BPh_4]^-$] were synthesized by cyclometalation of the [R-*iso*-BIPY−H]$^+$[OTF]$^-$ salts **1a**−**4a** ([R-*iso*-BIPY−H]$^+$ = *N*-(2-pyridyl)-R-pyridinium) with dimethylplatinum-μ-dimethyl sulfide dimer. X-ray crystal structures for **1b**, **2c**−**4c** as well as complexes having bipyridyl and cyclometalated phenylpyridine ligands, [(bipy)Pt(CH_3)(DMSO)]$^+$ (**5c**) and ($C_{11}H_8N$)Pt(CH_3)(DMSO) (**6c**), have been determined. The pyridinium-derived *N*-heterocyclic carbene complexes display localized C−C and C−N bonds within the pyridinium ligand that are indicative of carbene π-acidity. The significantly shortened platinum−carbon distance, for "parent" complex **1b**, together with NMR parameters and the ν(CO) values for carbonyl cations **1d**−**4d** support a degree of Pt−C10 multiple bonding, increasing in the order **3** < **4** < **2** < **1.** Degenerate DMSO exchange kinetics have been determined to establish the nature and magnitude of the *trans*-labilizing ability of these new *N*-heterocyclic carbene ligands. Exceptionally large second-order rate constants ($k_2 = 6.5 \pm 0.4$ $M^{-1}\cdot s^{-1}$ (**3c**) to 2300 ± 500 $M^{-1}\cdot s^{-1}$ (**1c**)) were measured at 25 °C using ^{1}H NMR magnetization transfer kinetics and variable temperature line shape analysis. These rate constants are as much as 4 orders of magnitude greater than those of a series of structurally similar cationic bis(nitrogen)-donor complexes [(N−N)Pt(CH_3)(DMSO)]$^+$ reported earlier, and a factor of 32 to 1800 faster than an analogous charge neutral complex derived from cyclometalated 2-phenylpyridine, ($C_{11}H_8N$)Pt(CH_3)(DMSO) ($k_2 = 0.21 \pm 0.02$ $M^{-1}\cdot s^{-1}$ (**6c**)). The differences in rate constant are discussed in terms of ground state versus transition state energies. Comparison of the platinum−sulfur distances with second order rate constants suggests that differences in the transition-state energy are largely responsible for the range of rate constants measured. The π-accepting ability and trans-influence of the carbene donor are proposed as the origin of the large acceleration in associative ligand substitution rate.

Introduction

The development of imidazolium-derived *N*-heterocyclic carbene ligands has had a major impact on catalysis,[1] including more active ruthenium olefin metathesis catalysts[2] and improved palladium and nickel catalysts for aryl halide cross-couplings.[1,3] Enhanced activity for catalysts bearing *N*-heterocyclic carbene ligands may be attributable to the strong σ-donating[4] and weak π-accepting properties of imidazole-2-ylidenes.[5] Carbene ligands derived from deprotonation of pyridinium rather than imidazolium cations would be stabilized by only one mesomeric nitrogen and thus should be even better σ-donors and π-acceptors.[6] These differences should magnify their trans-influence and trans-effect, making metal complexes based on this class of N-heterocyclic carbene ligand more substitutionally labile.

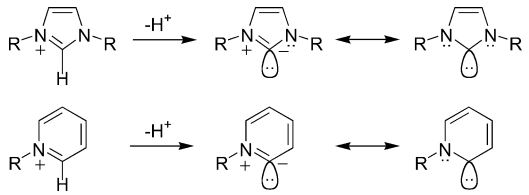

In recent model studies of the "Shilov cycle", the rate of benzene C−H bond activation by [(N−N)M(CH_3)L]$^+$ ((N−N) = α-diimine; M = Pt, Pd; L = H_2O, 2,2,2-trifluoroethanol =

(1) Herrmann, W. A. *Angew. Chem., Int. Ed. Engl.* **2002**, *41*, 1290−1309.
(2) Bielawski C. W.; Grubbs, R. H. *Angew. Chem. Int. Ed.* **2000**, *39*, 2903−2906. (b) Scholl, M.; Ding, S.; Lee, C. W.; Grubbs, R. H. *Org. Lett.* **1999**, *1*, 953−956. (c) Chaterjee, A. K.; Morgan, J. P.; Scholl, M.; Grubbs, R. H. *J. Am. Chem. Soc.* **2000**, *122*, 3783−3784. (d) Sanford, M. S.; Ulman, M.; Grubbs, R. H. *J. Am. Chem. Soc.* **2001**, *123*, 749−750. (e) Sanford, M. S.; Ulman, M.; Grubbs, R. H. *J. Am. Chem. Soc.* **2001**, *123*, 6543−6554.
(3) Littke, A. F.; Fu, G. C. *Angew. Chem., Int. Ed. Engl.* **2002**, *41*, 4176−4211. (b).
(4) Kocher, C.; Herrmann, W. A. *J. Organomet. Chem.* **1997**, *532* 261.
(5) Green, J. C.; Scurr, R. G.; Arnold, P. L.; Cloke, F. G. N. *J. Chem. Soc, Chem. Commun.* **1997**, 1963. (b) Boehme, C.; Frenking, G. *Organometallics* **1998**, *17*, 5801−5809.
(6) Gleiter, R.; Hoffmann, R. *J. Am. Chem. Soc.* **1968**, *90*, 5457−5460.

Scheme 1

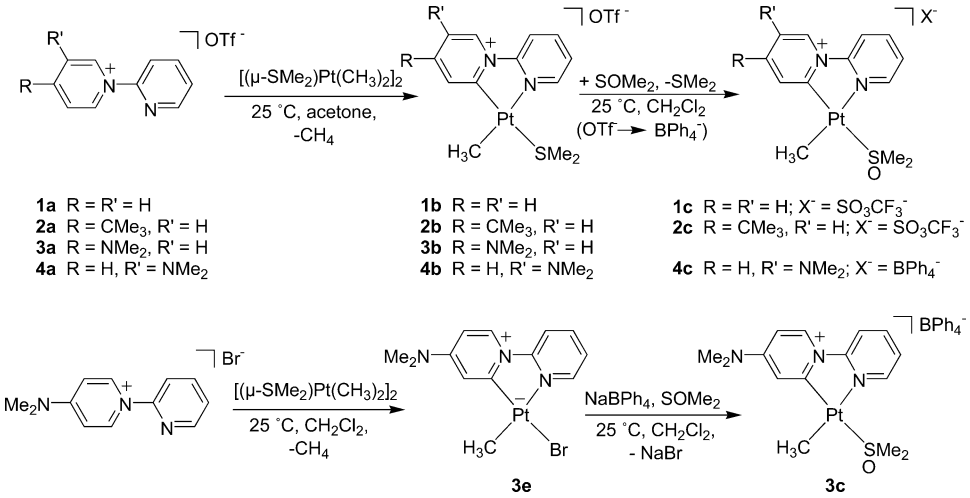

1a R = R' = H
2a R = CMe_3, R' = H
3a R = NMe_2, R' = H
4a R = H, R' = NMe_2

1b R = R' = H
2b R = CMe_3, R' = H
3b R = NMe_2, R' = H
4b R = H, R' = NMe_2

1c R = R' = H; $X^- = SO_3CF_3^-$
2c R = CMe_3, R' = H; $X^- = SO_3CF_3^-$
4c R = H, R' = NMe_2; $X^- = BPh_4^-$

3e **3c**

TFE) complexes in TFE solution was found to be strongly dependent on the position of the pre-equilibrium substitution of TFE for water.[7] Regardless of whether the rate-determining step is associative benzene displacement of TFE or oxidative addition of a benzene C−H bond, more electron-rich α-diimine ligands were found to decrease the thermodynamic preference for water binding and increase the overall rate of C−H activation. On the basis of these findings, we reasoned that electron-rich ligands capable of favoring the binding of TFE vs water and facilitating ligand substitution should enhance the propensity for a platinum(II) or palladium(II) complex to activate C−H bonds. We envisioned that the enhanced σ-donor and π-acceptor capabilities of pyridinium-derived *N*-heterocyclic carbenes might be ideal for facilitating substitution of a trans ligand.

We describe herein the synthesis of a series of square planar platinum(II) complexes having a new class of chelating pyridine/*N*-heterocyclic carbene donors, *N*-(2-pyridyl)-R-pyridine-2-ylidene (R = H, 4-*tert*-butyl, 4-dimethylamino, 5-dimethylamino).[8] (Because these ligands are isomers of 2,2′-bipyridyl, we abbreviate them as R-*iso*-BIPY.) To establish the σ- and π-bonding properties of this new ligand type, we determined the X-ray crystal structures for $[(R\text{-}iso\text{-BIPY})Pt(CH_3)(DMS)]^+$ and $[(R\text{-}iso\text{-BIPY})Pt(CH_3)(DMSO)]^+$ cations (DMS = dimethyl sulfide; DMSO = dimethyl sulfoxide), examined their NMR parameters and the carbonyl stretching frequencies for the corresponding methyl-carbonyl cations, and undertook studies of the kinetics of DMSO substitution trans to the carbene donor.

Results

Synthesis and Isolation of $[(R\text{-}iso\text{-BIPY})Pt(CH_3)L]^+$ Salts and Related Complexes. To avoid the need for preparation of a free, likely very reactive carbene, we designed pyridinium salts that would provide the desired carbene complexes upon cyclometalation.[9] Pyridinium salts **1a**−**4a** (Scheme 1) were prepared by heating the appropriately substituted pyridine with 2-pyridyl triflate at 150 °C under argon. These salts react with $[(\mu\text{-}SMe_2)Pt(CH_3)_2]_2$ in acetone or dichloromethane solution at room temperature, with liberation of one equivalent of methane, to give ∼50−90% isolated yields of the cyclometalated products **1b**−**4b**. Pyridinium salt **1a** reacts most rapidly giving an immediate color change and vigorous evolution of methane gas upon mixing. The dimethyl sulfide complexes **1b**−**4b** are useful synthons, providing access to the corresponding DMSO (**1c**, **2c**, **4c**) and carbonyl (**1d**−**4d**) complexes (Schemes 1 and 2).[10] The triflate salts were crystallized directly or were converted to tetraphenylborate salts (the bromide complex in the case of **3e**) by precipitation from methanol to generate more crystalline complexes suitable for X-ray structural analysis. All complexes can be handled and stored in air as solids at room temperature; however, solutions oxidize slowly in air.

Scheme 2

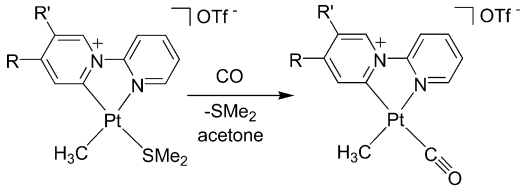

1b R = R' = H
2b R = CMe_3, R' = H
3b R = NMe_2, R' = H
4b R = H, R' = NMe_2

1d R = R' = H
2d R = CMe_3, R' = H
3d R = NMe_2, R' = H
4d R = H, R' = NMe_2

To compare the carbene complexes with closely related ones, $[(bipy)Pt(CH_3)(DMSO)]^+[BPh_4]^-$ (**5c**) and the cyclometalated 2-phenylpyridine adduct, $(C_{11}H_8N)Pt(CH_3)(DMSO)$ (**6c**), were synthesized. Protonolysis of $(bipy)Pt(CH_3)_2$ in the presence of DMSO and precipitation from methanol using $NaBPh_4$ provided **5c.** Complex **6c** was prepared analogously to **1c**−**4c**, using 2-phenylpyridine as the ligand precursor. The unstable dimethyl sulfide product was immediately trapped with DMSO and

(7) Zhong, H. A.; Labinger, J. A.; Bercaw, J. E. *J. Am. Chem. Soc.* **2002**, *124*, 1378−1399. (b) Ackerman, L. J.; Sadighi, J. P.; Kurtz, D. M.; Labinger, J. A.; Bercaw, J. E. *Organometallics* **2003,** *22*, 3884−3890.

(8) A few examples of monodentate pyridin-2-ylidene complexes of platinum and palladium have been prepared by protonation or methylation of the nitrogen of 2-pyridyl complexes. (a) Crociani, B.; Di Bianca, F.; Giovenco, A.; Scrivanti, A. *J. Organomet. Chem.* **1983**, *251*, 393−411. (b) Crociani, B.; Di Bianca, F.; Giovenco, A.; Scrivanti, A. *J. Organomet. Chem.* **1984**, *269*, 295−304. (c) There is also a report of 4-pyridyl complexes of rhodium and iridium that could be alkylated: Fanizzi, F. P.; Sunley, G. J.; Wheeler, J. A.; Adams, H.; Bailey, N. A.; Maitlis, P. M. *Organometallics* **1990**, *9*, 131.

(9) This strategy has been documented before: (a) McGuinnes, D. S.; Cavell, K. J.; Yates, B. F. *Chem, Commun.* **2001**, 355. (b) Herrmann, W. A.; Köcher, C.; Gooβen, L. J.; Artus, G. R. J. *Chem. Eur. J.* **1996**, *2*, 162. (c) Herrmann, W. A.; Kohl, F. J.; Scwarz, J. *Synthetic Methods of Organometallic and Inorganic Chemistry, Vol. 9*, Stuttgart; New York: Georg Thieme Verlag: New York: Thieme Medical Publishers: **2000**, p 84.

(10) Isolation of the dimethyl sulfide complex **3b** proved troublesome, so this complex was made in situ as a precursor to **3d**.

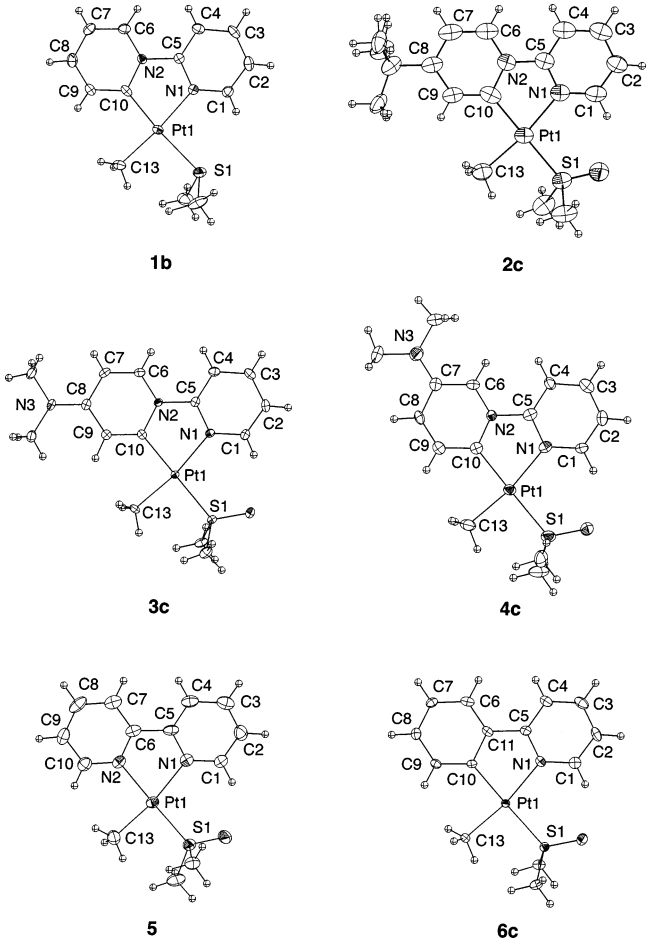

Figure 1.

Table 1. Selected Pt−X Bond Lengths [Å] for Complexes **1b**, **2c**, **3c**, **4c**, **5c**, and **6c**

	Pt–S(1)	Pt–C(13)	Pt–N(1)	Pt–C(10)
1b	2.3447(8)	2.037(3)	2.092(2)	1.959(3)
2c	2.2758(19)	2.077(7)	2.101(6)	1.996(7)
3c	2.2693(5)	2.046(2)	2.100(2)	2.011(2)
4c	2.2841(17)	2.050(6)	2.095(5)	2.004(6)
5c	2.1961(11)	2.053(4)	2.130(3)	2.066(3)[a]
6c	2.2759(9)	2.047(3)	2.114(3)	2.011(3)

[a] Pt−N(2).

isolated. Attempts to prepare the platinum−carbonyl complex $(C_{11}H_8N)Pt(CH_3)(CO)$ unfortunately proved unsuccessful.

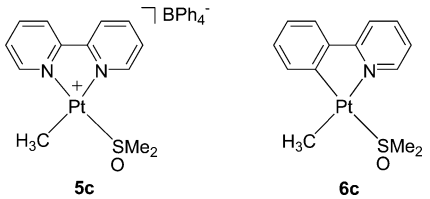

X-ray Crystal Structures, NMR, and Infrared Spectral Parameters. X-ray quality crystals of **1b** and **2c**−**6c** were grown by diffusion of petroleum ether or diethyl ether into their acetone or dichloromethane solutions. Their structures are shown in Figure 1. In all cases, the platinum methyl group is located trans to the pyridine nitrogen, and the dimethyl sulfide or dimethyl sulfoxide ligands trans to the carbene or phenyl donor. Table 1 gives ligand to platinum bond lengths for all complexes.

Table 2. Selected Ring Bond Lengths [Å] for Complexes **1b**, **3c**, **4c**, and **6c**

	N(2)–C(10)	C(10)–C(9)	C(9)–C(8)	C(8)–C(7)	C(7)–C(6)	C(6)–N(2)	$Me_2N–C_{Ar}$
1b	1.389(3)	1.410(4)	1.356(4)	1.393(4)	1.359(4)	1.369(2)	
3c	1.395(3)	1.376(3)	1.408(3)	1.423(3)	1.347(3)	1.370(3)	1.351(3)
4c	1.359(8)	1.405(9)	1.356(9)	1.394(9)	1.400(9)	1.355(8)	1.359(8)
6c	1.407(5)[a]	1.390(5)	1.386(5)	1.395(5)	1.376(5)	1.397(5)[b]	

[a] C(11)−C(10). [b] C(6)−C(11).

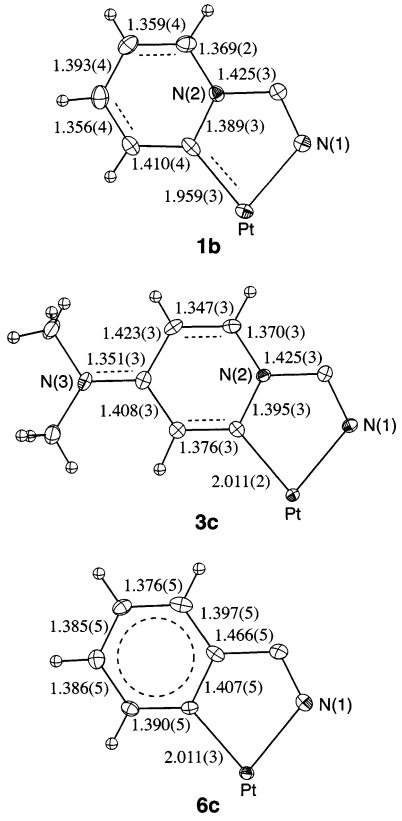

Figure 2.

Bonding of the sulfur and carbene donors with platinum is of particular interest. The Pt−S distances for complexes **2c**−**4c** and **6c** are indistinguishable (within 3σ (σ_{AVG}= 0.0012Å)), whereas in complex **5c** it is shorter by 0.08 Å. The Pt−C10 distances fall in the order **1b** < **2c** < **4c** < **3c** = **6c** < **5c** (**5c**, the bipy adduct, has no C10; the differences for **2c** and **4c** are comparable to the uncertainties). The Pt−C10 bond length of 1.959(3) Å for **1b** is significantly shorter than that of the typical sp^2-carbon−platinum single bond (2.01(1) Å),[11] whereas the values for **3c** and **6c** (2.011(2) and 2.011(3) Å, respectively) are closer. (It should be noted however that the ligand trans to C10 is DMS for **1b** but DMSO for **3c** and **6c**.)

The quality of the X-ray structure determinations for **1b**, **3c**, and **6c** also allows discrimination of C−C and C−N bond lengths within the ligand. Ring C−C and C−N distances for complexes **3c**, **4c**, **6c**, and **1b** are given in Table 2. Figure 2 shows the bond length patterns in **1b**, **3c** and **6c**.

(11) Several Pt−C (sp2) bond lengths trans to dimethyl sulfide or DMSO donors have been reported, with an average of 2.019 Å and maximum uncertainty of ± 0.007 Å. a) 2.036(7) and 2.010(7): Alibrandi, G.; Bruno, G.; Lanza, S.; Minniti, D.; Romeo, R.; Tobe, M. L. *Inorg. Chem.* **1987**, *26*, 185−190. (b) 2.018(5): Zucca, A.; Doppiu, A.; Cinellu, M. A.; Stoccoro, S.; Minghetti, G.; Manassero, M. *Organometallics* **2002**, *21*, 783−785. (c) 2.011(5) and 2.022(6): Unpublished results for (7,8-Benzoquinoline)Pt-$(CH_3)(SMe_2)$, CCDC# 170367.

Table 3. Selected Spectroscopic, Crystallographic, and Kinetics Parameters

	δ [ppm]	$^1J^{195}$Pt–^{13}C [Hz]	r(Pt–C) [Å]	ν(CO) [cm^{-1}][a]	k_2^{298} [M^{-1}s^{-1}][b]
1c	174.0	nd	nd	2099.4	382(50)
2c	172.2	1231.2	1.996(7)	2097.9	175(25)
3c	164.3	1203.8	2.011(2)	2088.9	6.51(36)
4c	160.9	1323.8	2.004(6)	2090.2	28.8(1.5)
6c	152.1	1070.9	2.011(3)	nd	0.21(2)

[a] For [OTf$^-$] salts of carbonyl adducts, **1d**−**4d**, in acetone-d_6. [b] In $C_2D_2Cl_4$.

Table 4. Second Order Rate Constants and Activation Parameters for Complexes **1c** and **2c** from Variable Temperature Line Shape Simulation

	[Pt][b]	[DMSO][b]	T range[c]	k_{obs}^{298} [d]	k_2^{298} [e]	k_i^{298} [f]	$\Delta H^{\ddagger}$[g]	$\Delta S^{\ddagger}$[h]
1c[a]	0.0308	0.0308	255−313	109			11.3	−11.3
	0.0416	0.0416	245−312	130			11.2	−11.3
	0.0525	0.0525	254−303	159	2300 ± 500	37	10.8	−12.3
1c[i]	0.0197	0.0197	314−347	20.5			10.7	−16.7
	0.0504	0.0504	304−338	36.3			10.2	−17.1
	0.0738	0.0738	304−336	40.8	382 ± 50	14	11.2	−13.6
2c[i]	0.0527	0.0264	314−348	8.4[j]			11.8	−14.6
	0.0527	0.0527	314−348	17.3			10.3	−18.2
	0.0527	0.0791	304−348	22.5			10.4	−17.3
	0.0527	0.1054	304−348	26.6	175 ± 25	8.3	10.3	−17.4

[a] In acetone-d_6. [b] M. [c] K. [d] s^{-1}, calculated. [e] M^{-1} s^{-1} slope from plot of k_{obs} vs [DMSO]. [f] s^{-1}, intercept ([DMSO] = 0) from plot of k_{obs} vs [DMSO]. [g] kcal/mol. [h] e. u. [i] In $C_2D_2Cl_4$. [j] excluded from determination of k_2.

Downfield ^{13}C NMR chemical shifts are characteristic features of carbene donors. Lappert and co-workers reported a range of δ = 175−218 ppm for a series of imidazolium-derived platinum−carbene complexes.[12] In complexes **2c**−**4c** and **6c**, the signal for the carbon bound directly to platinum can be unequivocally identified by the satellites due to the large ^{195}Pt−^{13}C coupling constants. ^{13}C{^{1}H} NMR spectra of complexes **2c**−**4c** have peaks in the range of δ = 160−175 ppm ($^1J_{Pt-C} \approx$ 1200−1300 Hz), whereas **6c** shows a chemical shift of δ = 152 ppm with a significantly smaller $^1J_{Pt-C}$ of 1071 Hz.[13] ^{13}C-{^{1}H} NMR data for complexes **2c**−**4c** and **6c** are included in Table 3, along with relevant crystallographic, infrared and kinetics data (see below).

At room temperature, complexes **1c**−**4c** show ^{1}H NMR spectra consistent with their solid-state structures. The $^2J_{Pt-H}$ satellites observed for the methyl signals (~81 Hz) are consistent with methyl trans to the pyridine nitrogen (as observed in the spectrum of **5c**). Notably, the 300 MHz ^{1}H NMR spectrum of **3c** shows inequivalent [N(CH_3)$_2$] resonances at room temperature, that coalesce at 70 °C.[14] In contrast complex **4c** shows one sharp [N(CH_3)$_2$] resonance at room temperature.

Ligand Substitution Kinetics. To investigate the *trans*-labilizing ability of these pyridine-2-ylidene ligands, DMSO exchange rates for complexes **1c**−**4c** and **6c** were measured in $C_2D_2Cl_4$ and acetone-d_6 solution, using magnetization transfer and variable temperature line shape simulation. Kinetic data are shown in Tables 4 and 5. Complexes **1c** and **2c** substitute most quickly, giving broad ^{1}H NMR spectra in the presence of free DMSO at room temperature. Simulation of their temperature-dependent spectra provided first-order rate constants (k_{obs}) and activation parameters. Plots of k_{obs} versus [DMSO] indicate an associative substitution mechanism with a first-order DMSO dependence[15] and a contribution from a DMSO-independent substitution pathway (k_i). Complexes **3c**, **4c**, and **6c** undergo slower associative DMSO exchange and were studied using magnetization transfer techniques at 298 K.[16] At the concentrations studied, the substitution rates display a linear dependence on DMSO concentration with no evidence for a DMSO-independent substitution path. The second-order rate constant for the parent pyridine-2-ylidene complex **1c** is 4 orders of magnitude greater than that measured for its structural isomer, bipy complex **5c**, and 3 orders of magnitude greater than its neutral 2-phenyl pyridine analogue **6c**.

Table 5. Second Order Rate Constants for Complexes **3c**, **4c**, **5**, and **6** from Magnetization Transfer Kinetics in $C_2D_2Cl_4$

	[Pt][a]	[DMSO][a]	k_{obs}^{298} [b]	k_2^{298} [c]	$[k_2^{298}]_{ave}$ [c]
3c	0.0240	0.0530	0.34	6.42	
	0.0570	0.1610	1.00	6.21	
	0.0760	0.1365	0.94	6.89	
	0.0760	0.2795	1.87	6.69	6.51 ± 0.36
4c	0.0387	0.1550	4.35	28.1	
	0.0388	0.0775	2.16	27.9	
	0.0389	0.3114	9.54	30.6	28.8 ± 1.5
5c[d]					0.16 ± 0.01
6c	0.0414	1.240	0.236	0.190	
	0.0413	2.063	0.419	0.203	
	0.0309	3.094	0.692	0.224	0.21 ± 0.02

[a] M. [b] s^{-1}. [c] M^{-1} s^{-1}. [d] In acetone-d_6. See ref 14a.

Discussion

Previous theoretical studies of complexes bearing imidazolium-derived *N*-heterocyclic carbenes suggest that they are primarily strong carbon σ-donor ligands.[5] Still unresolved, however, is whether π-bonding becomes important in the transition states and intermediates of catalytic reaction cycles, and has any consequence for catalytic activity. The major resonance contributors describing the interactions of a transition metal with *N*-heterocyclic carbenes derived from imidazolium (**A**) and pyridinium (**B**) cations are shown in Scheme 3. Analogy to the imidazolium-derived carbenes suggests that the σ-only form **B1** would be the most important contributor for pyridinium-derived carbenes, but as discussed below, our structural data and fast associative substitution kinetics suggest a significant role for π-acidity as well.

Structural and Spectroscopic Evidence. Bond length patterns in the X-ray structures of **3c** and **1b** demonstrate the importance of π−acidity of the carbene ligand. Resonance structures for complex **3c** (Scheme 4) reflect competition between the N pπ electrons of the dimethylamino substituent, the pyridinium N pπ electrons, and the dπ electrons of the platinum for the empty carbon pπ orbital. The X-ray structure of **3c** agrees best with the resonance depiction **3c′**, showing a platinum−carbon single bond with appropriate short/long alternations for double and single C−C bonds within the ring. The Pt−C10 distance (2.011(2) Å) indicates a relatively minor

(12) Cardin, D. J.; Cetinkay, B.; Lappert, M. F.; Randall, E. W.; Rosenberg, E. *J. Chem. Soc., Dalton Trans.* **1973**, *19*, 1982−1973.
(13) The lower solubility of **1c** prevented the determination of its ^1JPt−C coupling constant.
(14) The $\Delta G^{\ddagger}$ at 70 °C was estimated at 16.8 kcal/mol, and was found to be invariant to added DMSO.
(15) k_2 was determined from the slope of the k_{obs} versus [DMSO].
(16) Complex **6c** has a substitution rate nearly too slow to study by magnetization transfer at room temperature. Concentrated samples with several equivalents of DMSO were used to achieve reliably measurable rates of magnetization transfer.

Table 6. Crystal[a] and Refinement Data for Complexes **1b**, **2c**−**4c**, **5**, **6**

	1b $[BPh_4]^-$	**2c** $[OTf]^-$	**3c** $[BPh_4]^-$
empirical formula	$[C_{13}H_{17}N_2SPt]^+$ $[B(C_6H_5)_4]^- \cdot (C_3H_6O)$	$[C_{17}H_{22}N_2OSPt]^+$ $[SO_3CF_3]^- \cdot (C_6H_6)$	$[C_{15}H_{22}BN_3OSPt]^+$ $[B(C_6H_5)_4]^-$
formula weight	805.72	685.64	806.72
a, Å	11.0611(6)	21.8153(11)	11.0499(4)
b, Å	13.0966(7)	10.4419(5)	11.3835(4)
c, Å	14.2868(7)	22.0778(11)	14.9527(6)
α, deg	114.0150(10)		67.7790(10)
b, deg	91.9270(10)		74.5460(10)
γ, deg	111.0610(10)		88.1200(10)
volume, Å^3	1724.46(16)	5029.2(4)	1673.33(11)
Z	2	8	2
crystal system	triclinic	orthorhombic	triclinic
space group	P-1	*Pbcn*	P-1
d_{calc}, g/cm^3	1.552	1.811	1.601
θ range, deg	1.60 to 28.30	1.84 to 28.42	1.53 to 28.35
μ, mm^{-1}	4.163	4.291	4.291
abs. correction	none	none	none
GOF	1.215	1.86	1.365
R_1,[b] wR_2[c] [I>2σ(I)]	0.0244, 0.0509	0.0496, 0.0806	0.0203, 0.0470

	4c $[BPh_4]^-$	**5c** $[BPh_4]^-$	**6c**
empirical formula	$[C_{15}H_{22}N_3OSPt]^+$ $[B(C_6H_5)_4]^- \cdot (C_3H_6O)$	$[C_{13}H_{17}N_2OPtS]^+$ $[B(C_6H_5)_4]^- \cdot (C_3H_6O)$	$C_{14}H_{17}NOSPt$
formula weight	835.76	792.69	442.44
a, Å	11.1872(6)	23.0688(8)	10.3677(9)
b, Å	15.3712(8)	13.1532(5)	14.9165(13)
c, Å	20.8806(10)	23.9873(9)	17.3745(15)
α, deg			
β, deg	90.4650(10)	115.5560(10)	
γ, deg			
Volume, Å^3	3590.5(3)	6566.3(4)	2687.0(4)
Z	4	8	8
crystal system	monoclinic	monoclinic	orthorhombic
space group	$P2_1$	$P2_1/c$	*Pbca*
d_{calc}, g/cm^3	1.546	1.604	2.187
θ range, deg	1.65 to 28.39	1.71 to 28.60	2.34 to 28.49
μ, mm^{-1}	4.004	4.373	10.586
abs. correction	none	face-indexed Gaussian	face-indexed Gaussian
GOF	1.074	1.29	1.272
R_1,[b] wR_2[c] [I>2σ(I)]	0.0343, 0.0601	0.0359, 0.0538	0.0235, 0.0364

[a] 98(2) K. [b] $R_1 = \sum||F_o| - |F_c||/\sum|F_o|$. [c] $wR_2 = [\sum[w(F_o^2 - F_c^2)^2]/\sum[w(F_o^2)^2]]^{1/2}$.

Scheme 3

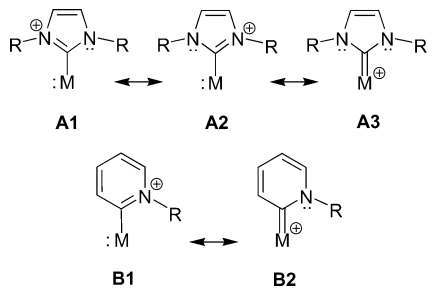

Scheme 4

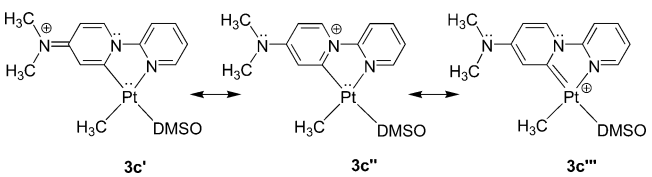

contribution from **3c‴**. In contrast, the absence of a dimethylamino substituent in **1b** leaves the empty carbene orbital to be stabilized only by interaction with the filled platinum d*π* orbital and the pyridinium N p*π* electrons. The former interaction results in the shortest Pt−C10 bond in the series (1.959(3) Å) and ligand C−C and C−N distances (Figure 2) consistent with significant contributions for both resonance structures **B1** and **B2** (Scheme 3). Both structures differ from that of metalated 2-phenylpyridine analogue **6c,** which shows delocalized bonding in the phenyl ring (Table 2, Figure 2), and a platinum−carbon distance (2.011(3) Å) not significantly different from that for **3c** (2.011(2) Å). The Pt−C10 distance of 1.959(3) Å for the "parent" example, **1b**, is significantly shorter than that expected for a single bond. We conclude, therefore, that the X-ray structural data support a degree of Pt−C10 *π*-bonding as depicted in resonance structure **B2** (Scheme 3).

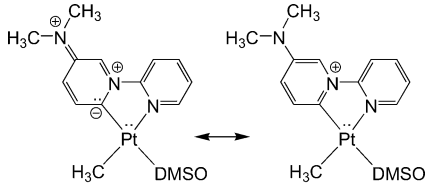

The NMR and infrared parameters for these complexes also suggest some modest Pt−C10 *π*-bonding. Although the ^{13}C NMR chemical shifts for the Pt-bonded carbon for **1c**−**4c** (*δ*

160.9−174.0) are significantly downfield of that for the metalated 2-phenylpyridine complex **6c** (δ 152.1), they are not so far downfield as those for the imidazolium-derived carbenes ($\delta = 175-218$) or alkylidenes ($\delta \geq 200$).[17] Moreover, the $^1J_{Pt-C}$ values for **2c**−**4c** are larger (1203.8−1323.8 Hz) than that for **6c** (1070.9 Hz), suggesting a higher Pt−C10 bond order for the (2-pyridyl)-R-pyridine-2-ylidene complexes. The carbonyl stretching frequencies for **1d**−**4d** lie in the order of increasing ν(CO): **3c** (2088.9 cm^{-1}) < **4c** (2090.2 cm^{-1}) < **2c** (2097.9 cm^{-1}) < **1c** (2099.4 cm^{-1}), approximately the order expected, as the "parent" ligand of **1c** should be most π acidic; **2c** and **4c** less so, because of the electron-releasing substituents; and **3c** least, because of the 4-amino nitrogen pπ donation (form **3c′**, Scheme 4).

An additional manifestation of the importance of resonance structure **3c′** (Scheme 4) is the measurable barrier to rotation about the $[(CH_3)_2N]-C_{Ar}$ bond in **3c** ($\Delta G^{\ddagger}_{343K} = 16.8$ kcal/mol). The much smaller barrier for **4c** is expected, because the analogous double bonded resonance structure (**4c′**) is disfavored by charge separation; the higher CO stretching frequency for **4d** vs. **3d** is also consistent with this argument.

Structural and Kinetics Evidence. Studies of degenerate DMSO exchange reveal effects of ligand bonding properties both on the ground state (trans-influence) and transition state (trans-effect). Romeo and co-workers have extensively studied associative, degenerate DMSO exchange at cationic alkyl platinum centers.[18] For $[(N-N)Pt(CH_3)(DMSO)]^+$ complexes (N−N = a bis(nitrogen donor)) in acetone-d_6 solution second-order rate constants range from $[(9.49 \pm 0.05) \times 10^{-6}\ M^{-1}s^{-1}]$ for (N−N) = tetramethylethylenediamine to $[0.920\ M^{-1}\ s^{-1}]$ for (N−N) = 1,4-dicyclohexyl-1,4-diazabutadiene.[18a,19] Romeo's findings can serve as a basis for comparison, in attempting to quantify the extent to which these new pyridinium-derived *N*-heterocyclic carbene ligands accelerate ligand substitution.

Langford and Gray[20] and others[21] have suggested that strong σ-bonding between a ligand and the platinum 6s and 5p orbitals limits the availability of those metal-based orbitals for interacting with the trans-ligand, thus weakening its bonding interaction, a phenomenon termed "trans-influence." Experimentally, stronger σ-donation results in greater trans-influence, with carbon and hydride donors being among the strongest.[21]

π-Bonding, on the other hand, generally exerts its greatest influence in the transition state structure, with ligands of greater π-acid character accelerating associative ligand substitution.[21] The importance of this π-bonding to the relative energies of similar trigonal bipyramidal structures can be understood by examining the equatorial orbital interactions. A qualitative

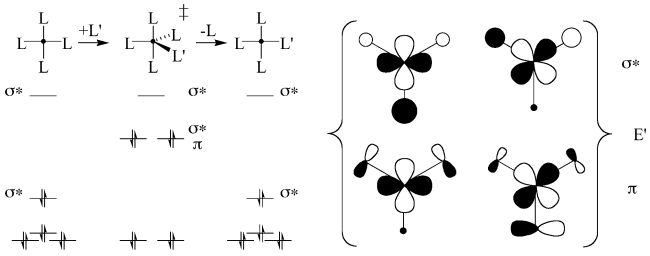

Figure 3.

diagram of the frontier orbitals of the square planar ground state and trigonal bipyramidal transition state on an associative substitution pathway is shown in Figure 3. In this representation, π-acceptors lower the transition state energy, while strong σ-donors raise it.

Relative ligand trans-influence can be measured by examining the bond lengths of the ligand trans to the *N*-heterocyclic carbene ligand.[21] Thus, any differences in the platinum−sulfur bond lengths among the series **2c**−**6c** should allow an assessment of relative ground-state energies on the associative substitution reaction profile. X-ray crystal structures of the DMSO cations **2c**−**4c**, **6c** show very similar platinum−sulfur distances (Table 1), whose average of 2.274 Å is significantly longer (by about 0.08 Å) than the Pt−S distance (2.1961(11) Å) for the bipy complex **5c**. This indicates, as expected, a substantially greater trans-influence for ligands having a Pt−C bond (**2c**−**4c**, **6c**) as compared with a Pt−N bond. The similarity between the platinum−sulfur distances in **2c**−**4c** and **6c** is important and suggests that formally neutral *N*-heterocyclic carbene and anionic sp^2-hybridized phenyl carbon donors have a similar trans-influence.[22] This property is maintained despite the lower basicity of a carbene carbon, and is likely the result of the π-acceptor character and greater bond order documented above. However, this is not reflected in the substitution rates: that for **6c** is 1−3 orders of magnitude lower than those for the carbene complexes.[23]

We conclude, therefore, that the large acceleration of ligand substitution for **1c**−**4c** compared to **6c**, is primarily due to stabilization of the transition state energies. This result can be rationalized using the orbital diagram shown above in Figure 3 where both π-acceptors and weaker σ-donors stabilize the transition structure. The trend in the associative DMSO substitution rates (**1c** > **2c** > **4c** > **3c**) parallels the relative ground state π-acidities for the *N*-heterocyclic carbene ligands.

The distinctive σ-donating/π-accepting characteristics of carbene-donor ligands are undoubtedly quite relevant to their increasing role in homogeneous catalysis. Structural, spectroscopic and kinetics evidence cited here indicates that it is an augmentation of π-accepting capability that distinguishes the pyridine-2-ylidene donors from their formally anionic phenyl analogues, and make them particularly well suited for accelerating associative ligand substitution. We are currently working on exploiting this property for enhancing C−H activation and related chemistry.

(17) Crabtree, R. H. *The Organometallic Chemistry of the Transition Metals*; John Wiley & Sons: 2001, pp 265, 298.
(18) Romeo, R.; Scolaro, L. M.; Nastasi, N.; Arena, G. *Inorg. Chem.* **1996**, *35*, 5087−5096. (b) Romeo, R.; Nastasi, N.; Scolaro, L. M.; Plutino, M. R.; Albinati, A.; Macchioni, A. *Inorg. Chem.* **1998**, *37*, 5460−5466. (c) Romeo, R.; Fenech, L.; Scolaro, L. M.; Albinati, A.; Macchioni, A.; Zuccaccia, C. *Inorg. Chem.* **2001**, *40*, 3293. (d) Romeo R.; Fenech L.; Carnabuci, S.; Plutino, M. R.; Romeo, A. *Inorg. Chem.* **2002**, *41*, 2839−2847.
(19) [(2,9-Dimethylphenanthroline)platinum(methyl)(DMSO)]$^+$ had a substitution rate much faster than the all other complexes in Romeo's study, but it was determined to substitute by a different mechanism.
(20) Langford, C. H.; Gray, H. B. *Ligand Substitution Processes*; W. A. Benjamin, Inc.: New York, 1966.
(21) Spessard, G. O.; Miessler, G. L. *Organometallic Chemistry*, Prentice Hall, Upper Saddle River, New Jersey, 1997. (b) Basolo, F.; Pearson, R. G. *Prog. Inorg. Chem.* **1962**, *4*, 381. (c) Wendt, O. F. *Platinum(II) and Palladium-(II) Complexes with Group 14 and 15 Donor Ligands*, Ph.D. Thesis, **1997,** Lund University, Lund, Sweden. (d) Crabtree, R. H. *The Organometallic Chemistry of the Transition Metals*; John Wiley & Sons: New York, 2001.
(22) Crociani et. al. inferred from ν(Pt−Cl) stretching frequencies that the trans-influence of 2-pyridyl is less than its ylidene analogue. ref 8b.
(23) Romeo[18a] has observed that stronger σ-donation need not result in a greater *trans*-effect. In the context of the bonding model described in Figure 3, this would depend on the relative importance of σ-antibonding interactions in the ground and transition states for substitution.

Experimental Section

General Methods. All air and/or moisture sensitive compounds were manipulated using standard Schlenk techniques or in a glovebox under a nitrogen atmosphere, as described previously.[24] 4-*tert*-butylpyridine, 4-(dimethylamino)pyridine, and pyridine were purchased from Aldrich, distilled from CaH_2 and stored under argon. 2-phenylpyridine, 2,2′-bipyridyl, and sodium tetraphenylborate were purchased from Aldrich and used as received. 3-(dimethylamino)pyridine,[25] 2-pyridyl triflate,[26] and $[(\mu\text{-}SMe_2)Pt(CH_3)_2]_2$[27] were prepared as described previously. $C_2D_2Cl_4$ and acetone-d_6 were purchased from Cambridge Isotope Laboratories, distilled from CaH_2 and $CaSO_4$, respectively, and stored under argon. Dimethyl sulfoxide used in kinetic experiments was passed through an activated alumina column and stored under argon. NMR spectra were recorded on a Varian ^{UNITY}INOVA 500 (499.853 MHz for ^{1}H) spectrometer.

Magnetization Transfer Experiments and Line Shape Analysis Experiments. Both types of experiments were carried out in J. Young NMR tubes under 1 atm of argon. Solutions were prepared in 1.0 mL volumetric flasks. Reaction temperatures were determined by measuring the peak separation of an ethylene glycol or methanol standard before and after the experiment at each temperature.

Magnetization transfer experiments were conducted at 25 °C by inversion of the signal for free DMSO using a selective DANTE inversion sequence.[28] Relaxation times (T_1) for the resonances of interest were measured before the magnetization transfer experiment using the inversion recovery method. Signals for free and bound DMSO were integrated at delay times τ and fit to a two-site exchange model using the program CIFIT. (Figure 4). Pseudo-first-order rate constants obtained from these fits were plotted versus DMSO concentration. All plots showed a linear dependence on DMSO concentration and a zero intercept within experimental error (Figure 5).

Variable temperature line shape data for complexes **1c** and **2c** were recorded in 10-degree increments from the static spectrum (−40 °C) until the boiling point of the solvent or temperature limitation of the NMR probe (<100 °C). In all cases, a coalescence point was reached. Line broadening of the platinum bound DMSO was used to calculate first-order rate constants in the slow exchange region according to eq 1.[29] The temperature dependence of the ^{195}Pt satellites of the platinum-

$$k_{obs}{}^{t} = 1/\tau_t = \pi(w_t{}^{1/2} - w_o{}^{1/2}) \qquad (1)$$

bound DMSO signal introduces error in the measured line widths at half-height ($w_t{}^{1/2}$). Spectra with significant contributions to the width at half-height from the platinum satellites were discarded in the Eyring analysis. Eyring plots of these pseudo-first-order rate constants (Figure 6) provided a method of determining pseudo-first-order rate constants at 298 K ($k_{obs}{}^{298}$). These rate constants were plotted versus DMSO to determine rate constants for the DMSO dependent (k_2) and independent (k_i) substitution paths.

Pyridinium Salts. All pyridinium triflate salts were prepared by a procedure analogous to the one detailed for **2a** below, with exceptions noted.

***N*-(2-Pyridyl)-4-*tert*-butylpyridinium Triflate.** (**2a**) 2-Pyridyl triflate (7.33 g, 32.3 mmol) and 4-*tert*-butylpyridine (8.73 g, 64.5 mmol) were combined under argon in a Teflon-stoppered Schlenk tube equipped with a stir bar. The solution was degassed, sealed under vacuum, and heated to 140 °C. After stirring overnight (~12 h), the colorless solution turned black and upon cooling partially solidified. Dissolving the mixture in CH_2Cl_2 and addition of diethyl ether precipitated a dark purple solid that was isolated on a glass frit. Several recrystallizations from hot ethyl acetate provided 6.88 g (59%) of **2a** as purple crystals. ^{1}H NMR (300 MHz, $CDCl_3$): δ = 1.47 (s, 9H, $C(CH_3)_3$), 7.64 (dd, 1H, ^3J = 7.7 Hz, ^3J = 4.9 Hz), 8.15 (ddd, 1H, ^3J = 8.1 Hz, ^3J = 8.1 Hz, ^4J = 1.6 Hz), 8.24 (d, 2H, ^3J = 7.1 Hz), 8.20 (d, 1H, ^3J = 8.2 Hz), 8.65 (dd, 1H, ^3J = 2.8 Hz, ^4J = 1.6 Hz), 9.58 (d, 2H, ^3J = 7.1 Hz); ^{13}C{^{1}H} (75 MHz, $CDCl_3$): δ = 24.3, 32.4, 122.1, 131.5, 132.7, 148.78, 148.79, 148.9, 158.2, 185.8; Anal. Calcd for $C_{15}H_{17}F_3N_2O_3S$: C, 49.72; H, 4.73; N, 7.73. Found: C, 49.65; H, 4.66; N, 7.66.

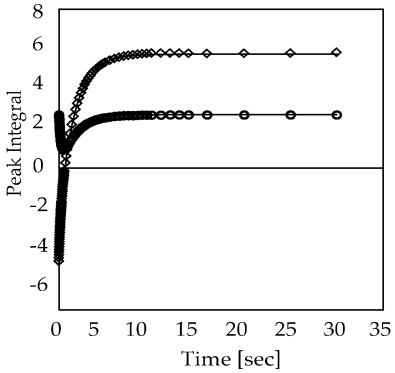

Figure 4. Magnetization transfer data for **(4c)** at 298 K in CD_2Cl_4. (○) Bound DMSO. (◇) Free DMSO. (−) The best fit line from a two-site exchange model. k_{obs} = 2.16 s^{-1}; k_2 = 27.9 $M^{-1}s^{-1}$.

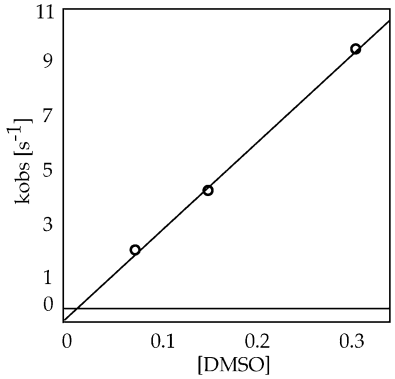

Figure 5. k_{obs} versus [DMSO] for (**4c**) at 298 K in $C_2D_2Cl_4$. k_2 = 27.9 M^{-1} s^{-1}.

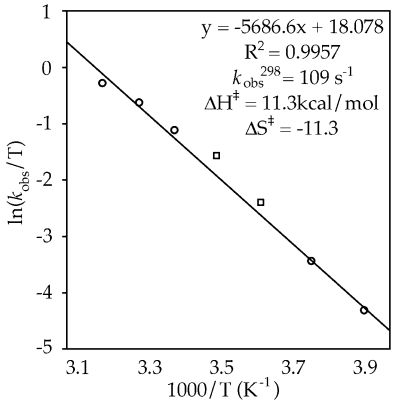

Figure 6. Eyring plot for (**1c**) in acetone-d_6 from 255 to 313 K. The value for k_2 was calculated from the linear best-fit at 298 K. (○) $k_{obs}{}^{T}$, (□) Data points excluded due error from ^{195}Pt satellites.

(24) Burger, B. J.; Bercaw, J. E. *New Developments in the Synthesis, Manipulation, and Characterization of Organometallic Compounds*; Wayda, A., Darensbourg, M. Y., Eds.; American Chemical Society: Washington, DC, 1987; Vol. 357.
(25) Giam, C. S.; Hauck, Albert E. *Organic Preparations and Procedures International*; **1977**, *9*(1), 9−11.
(26) Keumi, Takashi; Yoshimura, Kiichiro; Shimada, Masakazu; Kitajima, Hidehiko. *Bull. Chem. Soc. Jpn.* **1988**, *61*(2), 455−9.
(27) Hill, G.S.; Irwin, M.J.; Levy, C.J.; Rendina, L.M.; Puddephatt, R.J. *Inorg. Synth.* **1998**, *32*, 149−153.
(28) Morris, G. A.; Freeman, R. *J. Magn. Reson.* **1978**, *29*, 433−462.
(29) Günther, H. *NMR Spectroscopy, Second Edition*; John Wiley & Sons Limited: West Sussex, England, 1995; pp. 335−346.

***N*-(2-Pyridyl)-pyridinium Triflate (1a).** 2-Pyridyl triflate (7.33 g, 32.3 mmol) and pyridine (10.21 g, 129.1 mmol) were stirred for 18 h at 140 °C. The crude material was recrystallized from $CHCl_3$ and diethyl ether. 1.942 g (20%) of **1a** as pink plates were obtained. ^{1}H NMR (300 MHz, CD_2Cl_2): δ = 7.71 Hz (dd, 1H, ^3J = 7.7 Hz, ^3J = 4.9 Hz), 8.23 (ddd, 1H, ^3J = 8.2 Hz, ^3J = 8.2 Hz, ^4J = 1.6 Hz), 8.35 (t, 2H, ^3J = 7.7 Hz), 8.51 (d, 1H, ^3J = 8.2 Hz), 8.68−8.75 (m, 2H), 9.74 (d, 2H, ^3J = 6.0 Hz); ^{13}C{^{1}H} (75 MHz, CD_2Cl_2): δ = 118.0, 127.7, 129.2, 141.8, 142.5 (br, 2C), 148.4, 150.3; Anal. Calcd for $C_{11}H_9F_3N_2O_3S$: C, 43.14; H, 2.96; N, 9.15. Found: C, 43.35; H, 2.99; N, 9.02.

***N*-(2-Pyridyl)-4-(dimethylamino)-pyridinium Triflate (3a).** 2-Pyridyl triflate (2.932 g, 12.9 mmol) and 4-(dimethylamino)pyridine (3.154 g, 25.8 mmol) were stirred 5 h at 150 °C. The crude material was recrystallized from ethanol and diethyl ether giving **3a** as a high yield of pink plates. ^{1}H NMR (300 MHz, $CDCl_3$): δ = 3.36, 8.23 (ddd, 1H, ^3J = 8.2 Hz, ^3J = 8.2 Hz, ^4J = 1.6 Hz), 7.14 (d, 2H, ^3J = 8.2), 7.45 (ddd, 1H, ^3J = 7.1 Hz, ^3J = 4.9 Hz, ^4J = 1.1 Hz), 7.92 (d, 1H, ^3J = 8.2 Hz), 8.02 (ddd, 1H, ^3J = 6.9 Hz, ^3J = 6.9 Hz, ^4J = 1.9 Hz), 8.53 (d, 2H, ^3J = 4.8 Hz), 8.91 (d, 2H, ^3J = 7.7 Hz); ^{13}C{^{1}H} (125 MHz, $CDCl_3$): δ = 40.7, 108.4, 114.6, 124.7, 138.3, 140.6, 149.2, 150.5, 157.3; Anal. Calcd for $C_{13}H_{14}F_3N_3O_3S$: C, 44.70; H, 4.04; N, 12.03. Found: C, 44.63; H, 4.01; N, 11.97.

***N*-(2-Pyridyl)-5-(dimethylamino)-pyridinium Triflate (4a).** 2-Pyridyl triflate (4.279, 18.8 mmol) and 3-(dimethylamino)pyridine (2.303 g, 18.8 mmol) were heated to 140 °C overnight. Addition of diethyl ether to a CH_2Cl_2 solution of the crude product caused a black oil to separate. Decanting the solvent and removing the volatiles in vacuo provided a dark brown solid that was recrystallized from CH_2Cl_2 and diethyl ether to give 3.444 g (52%) of **4a** as very dark yellow crystals. ^{1}H NMR (300 MHz, $CDCl_3$): δ = 3.23 (s, 6H, N(CH_3)$_2$), 7.64 (dd, 1H, ^3J = 7.7 Hz, ^3J = 4.7 Hz), 7.79 (dd, 1H, ^3J = 9.1 Hz, ^3J = 3.0 Hz), 7.95 (dd, 1H, ^3J = 8.8 Hz, ^3J = 6.0 Hz,), 8.17 (ddd, 1H, ^3J = 6.3 Hz, ^3J = 6.3 Hz, ^4J = 1.7 Hz), 8.31 (d, 1H, ^3J = 8.2 Hz), 8.57 (m, 1H), 8.63 (dd, 1H, ^3J = 2.8 Hz, ^4J = 1.7 Hz), 8.69 (d, 1H, ^3J = 6.0 Hz); ^{13}C{^{1}H} (75 MHz, $CDCl_3$): δ = 40.5, 100.1, 118.3, 123.9, 127.0, 127.5, 128.1, 128.4, 141.5, 148.7, 149.5; Anal. Calcd for $C_{13}H_{14}F_3N_3O_3S$: C, 44.70; H, 4.04; N, 12.03. Found: C, 44.57; H, 4.02; N, 11.93.

Cylclometalation of the Pyridinum Salts 1a−4a. All of the carbene complexes were prepared and purified according to the procedure described for **1b** below. Complex **3b** was only prepared in situ and was immediately converted to **3d**, and isolated as a carbonyl cation.

[(*iso*-BIPY)Pt(CH$_3$)(DMS)]$^+$ [OTF]$^-$ (1b). [(μ-SMe$_2$)Pt(CH$_3$)$_2$]$_2$ (0.984 g, 1.71 mmol) was added, in one portion, to a solution of *N*-(2-pyridyl)-pyridinium triflate (**1a**) (1.049 g 3.43 mmol) in 50 mL of methylene chloride under argon purge. Evolution of methane was immediately observed upon mixing, and the solution quickly became a yellow orange color. After stirring for 1 h a small amount of diethyl ether was slowly added to precipitate a dark solid. After stirring for 30 min the solution was cannula-filtered to remove the dark solids and the filtrate concentrated. Addition of diethyl ether precipitated a mustard colored powder which was isolated on a glass frit and dried under vacuum. Yield 1.887 g (95%). ^{1}H NMR (500 MHz, acetone-d_6) δ = 1.17 (s, 3H, ^{2}JPt−H = 82.04 Hz, Pt−CH_3), 2.60 (br s, 6H, ^{3}JPt−H = ∼28 Hz S(CH_3)$_2$), 7.88 (ddd, 1H, ^3J = 6.9 Hz, ^3J = 6.9 Hz, ^4J = 1.4 Hz), 8.03 (ddd, 1H, ^3J = 5.5 Hz, ^3J = 5.5 Hz, ^4J = 0.9 Hz), 8.22−8.42 (m, 2H), 8.63 (ddd, 1H, ^3J = 7.3 Hz, ^3J = 7.3 Hz, ^4J = 1.4 Hz), 8.7 (d, 1H, ^3J = 8.4 Hz), 9.22 (br d, 1H ^3J = 5.06 Hz), 9.6 (br d, 1H ^3J = 6.14 Hz); ^{13}C{^{1}H} (125 MHz, acetone-d_6): δ = −9.40 (^{1}JPt−C = 792.2, Pt−CH_3), 20.39, 116.8, 122.5, 128.8, 133.9 (*J*Pt−C = 113.8 Hz), 140.5 (*J*Pt−C = 34.7 Hz), 143.2, 144.42 (*J*Pt−C = 53.7 Hz), 147.8, 157.0, 176.1 (^{1}JPt−C = 1317.1 Hz, Pt−C_{car}); Anal. Calcd for $C_{14}H_{17}F_3N_2O_3PtS_2$: C,29.12; H, 2.97; N, 4.85. Found: C, 29.05; H, 2.88; N, 4.77.

[(4-*tert*-Butyl-*iso*-BIPY)Pt(CH$_3$)(DMS)]$^+$ [OTF]$^-$ (2b). [(μ-SMe$_2$)-Pt(CH$_3$)$_2$]$_2$ (0.954 g, 1.66 mmol) and *N*-(2-pyridyl)-4-*tert*-butyl-pyridinium triflate (**2a**) (1.203 g, 3.32 mmol) were allowed to react to yield 1.904 g (94%) of **2b** as a yellow powder. ^{1}H NMR (300 MHz, CD_2Cl_2) δ = 1.22 (s, 3H, ^{2}JPt−H = 81.3 Hz Pt−CH_3), 1.44 (s, 9H), 2.52 (br s, 6H, ^{3}JPt−H = ∼32 Hz, S(CH_3)$_2$), 7.75−7.81 (m, 2H), 8.28 (d, 1H, ^4J = 2.2 Hz, ^{3}JPt−H = 54.9 Hz), 8.46 (ddd, 1H, ^3J = 7.1 Hz, ^3J = 7.1 Hz, ^4J = 1.7 Hz), 8.63 (d, 1H, ^3J = 8.2 Hz), 9.09 (dd, 1H, ^3J = 5.5 Hz, ^3J = 1.1 Hz, ^{3}JPt−H = 7.1 Hz), 9.43 (d, 1H, ^3J = 7.7 Hz); ^{13}C{^{1}H} NMR (125 MHz, CD_2Cl_2): δ = −9.31 (^{1}JPt−C = 791.8 Hz, Pt−CH_3), 20.77, 30.14, 37.08, 116.2, 120.5, 127.6, 129.9 (*J*Pt−C = 120.8 Hz), 138.7 (*J*Pt−C = 39.5 Hz), 142.8, 146.7, 156.3 (*J*Pt−C = 49.6 Hz), 169.0 (*J*Pt−C = 49.6 Hz), 179.2 (^{1}JPt−C = 1321.6 Hz, Pt−C_{car}); Anal. Calcd for $C_{18}H_{25}F_3N_2O_3PtS_2$: C, 33.28; H, 3.88; N, 4.31. Found: C, 34.03; H, 4.08; N, 4.16.

[(5-(Dimethylamino)-*iso*-BIPY)Pt(CH$_3$)(DMS)]$^+$ [OTF]$^-$ (4b). (μ-SMe$_2$)Pt(CH$_3$)$_2$]$_2$ (0.758 g, 1.318 mmol) and *N*-(2-pyridyl)-3-(dimethylamino)-pyridinium triflate (**4a**) (0.921 g 2.64 mmol) were allowed to react to yield 1.176 g (72%) of **4b** as a yellow powder. ^{1}H NMR (300 MHz, CD_2Cl_2) δ = 1.15 (s, 3H, ^{2}JPt−H = 80.85 Hz, Pt−CH_3), 2.51 (s, 6H, ^{3}JPt−H = 31.5 Hz, S(CH_3)$_2$), 3.14 (s, 6H, NMe_2), 7.53 (dd, 1H, ^3J = 9.3 Hz, ^4J = 2.8 Hz, *J*Pt−H = 6.0 Hz), 7.76 (ddd, 1H, ^3J = 5.5 Hz, ^3J = 5.5 Hz, ^4J = 1.1 Hz), 8.06 (d, 1H, ^3J = 9.3 Hz, *J*Pt−H = 23.6 Hz), 8.40 (d, 1H, ^3J = 2.75 Hz, *J*Pt−H = 4.2 Hz), 8.51 (ddd, 1H, ^3J = 7.7 Hz, ^3J = 7.7 Hz, ^4J = 1.6 Hz), 8.67 (d, 1H ^3J = 8.24 Hz), 9.07 (dd, 1H ^3J = 6.04 Hz, ^4J = 1.1 Hz); ^{13}C{^{1}H} NMR (125 MHz, CD_2Cl_2): δ = −10.31 (^{1}JPt−C = 789.2 Hz, Pt−CH_3), 20.77, 40.5, 116.8 (*J*Pt−C = 13.6 Hz), 120.3 (*J*Pt−C = 40.1 Hz), 127.7, 128.8 (*J*Pt−C = 117.5 Hz), 132.5 (*J*Pt−C = 117.5 Hz), 142.4, 145.5, 146.2, 156.7 (*J*Pt−C = 51.2 Hz), 176.1 (^{1}JPt−C = 1323.3 Hz, Pt−C_{car}); Anal. Calcd for $C_{16}H_{22}F_3N_3O_3PtS_2$: C,30.97; H, 3.57; N, 6.77. Found: C, 30.92; H, 3.54; N, 6.58.

Substitution of Dimethyl Sulfide by Dimethyl Sulfoxide. The dimethyl sulfide complex is mixed with sufficient DMSO (∼20 eq) to fully dissolve the sample, and is left stirring under vacuum for 1 h. The residue is then dissolved in a small amount of dichloromethane under argon, and the product precipitated with diethyl ether, filtered and dried under vacuum.

[(*iso*-BIPY)Pt(CH$_3$)(DMSO)]$^+$ [OTf]$^-$ (1c). The reaction was carried out according to the above procedure. [(*iso*-BIPY)Pt(CH$_3$)-(DMS)]$^+$[OTf]$^-$ (**1b**) (0.257 g, 0.445 mmol), DMSO (0.63 mL, 8.9 mmol, 20 eq); yield 93%. ^{1}H NMR (300 MHz, $CDCl_3$) δ = 0.89 (s, 3H, ^{2}JPt−H = 80.2 Hz, Pt−CH_3), 3.34 (br s, 6H, ^{3}JPt−H = 21.1 Hz, S(CH_3)$_2$), 7.74 (at, 1H, ^3J = 6.2 Hz), 7.98 (at, 1H, ^3J = 6.2 Hz), 8.10 (at, 1H, ^3J = 7.51 Hz), 8.25 (d, 1H, ^3J = 8.0 Hz, *J*Pt−H = 23.9 Hz), 8.48 (at, 1H, ^3J = 7.73 Hz), 9.01 (d, 1H, ^3J = 8.7 Hz), 9.85 (d, 1H ^3J = 5.55 Hz), 10.03 (d, 1H ^3J = 5.55 Hz); ^{13}C{^{1}H} (125 MHz, acetone-d_6): δ = −11.20 (^{1}JPt−C = 757.8 Hz, Pt−CH_3), −43.15 (Pt−OS-(CH_3)$_2$), 116.1, 123.3, 127.6, 133.4, 140.2, 143.0, 144.1, 150.8, 156.4, 174.0; Anal. Calcd for $C_{14}H_{17}F_3N_2O_4PtS_2$: C,28.33; H, 2.89; N, 4.72. Found: C, 28.07; H, 2.81; N, 4.58.

[(4-*tert*-Butyl-*iso*-BIPY)Pt(CH$_3$)(DMSO)]$^+$ [OTf]$^-$ (2c). The reaction was carried out according to a procedure similar to the above. [(*tert*-butyl-*iso*-BIPY)Pt(CH$_3$)(DMS)]$^+$[OTf]$^-$ (**2b**) (0.122 g, 0.199 mmol), DMSO (0.30 mL, 3.98 mmol, 20 eq); yield 107 mg (86%). ^{1}H NMR (300 MHz, CD_2Cl_2) δ = 0.90 (s, 3H, ^{2}JPt−H = 80.4 Hz, Pt−CH_3), 1.44 (s, 3H, *tert*-Bu), 3.30 (s, 6H, ^{3}JPt−H = 21.2 Hz, OS(CH_3)$_2$), 7.74 (at, 1H, ^3J = 6.8 Hz), 7.87 (dd, 1H, ^3J = 7.1 Hz, ^4J = 2.2 Hz), 8.25 (d, 1H, ^3J = 2.3 Hz, *J*Pt−H = 26.1 Hz), 8.43 (ddd, 1H, ^3J = 7.7 Hz, ^3J = 7.7 Hz, ^2J = 1.8 Hz), 8.68 (d, 1H, ^3J = 8.6 Hz), 9.87 (d, 1H, ^3J = 7.0 Hz), 9.88 (dd, 1H, ^3J = 5.8 Hz, ^4J = 1.4 Hz); ^{13}C{^{1}H} (125 MHz, CD_2Cl_2): δ = −10.2 (^{1}JPt−C = 757.4 Hz, Pt−CH_3), 30.2, 37.2, 44.3 (−43.15, ^{1}JPt−C = 44.5 Hz, (Pt−OS(CH_3)$_2$), 116.1, 121.5 (^{1}JF−C = 321.9 Hz, $F_3CSO_3^-$) 121.9, 127.4, 130.1 (*J*Pt−C = 112.4 Hz), 139.2 (*J*Pt−C = 35.4 Hz), 143.3, 151.2, 156.1 (*J*Pt−C = 47.7 Hz), 169.6-(*J*Pt−C = 47.7 Hz), 172.2 (^{1}JPt−C = 1231.2 Hz, Pt−C); Anal. Calcd for $C_{18}H_{25}F_3N_2O_4PtS_2$: C, 33.28; H, 3.88; N, 4.31. Found: C, 34.03; H, 4.08; N, 4.16.

[(5-(Dimethylamino)-*iso*-BIPY)Pt(CH_3)(DMSO)]$^+$ [OTF]$^-$ (4c). The reaction was carried out according to the above procedure to yield 1.176 g (72%) of **4c** as an orange powder. ^{1}H NMR (300 MHz, CD_2Cl_2) δ = 1.15 (s, 3H, ^2JPt−H = 81.0 Hz, Pt−CH_3), 2.51 (s, 6H, ^3JPt−H = 31.7 Hz, OS(CH_3)$_2$), 3.14 (s, 6H, N(CH_3)$_2$), 7.53 (dd, 1H, ^3J = 9.3 Hz, ^4J = 2.8 Hz, JPt−H = 6.4 Hz), 7.76 (ddd, 1H, ^3J = 5.5 Hz, ^3J = 5.5 Hz, ^4J = 1.1 Hz), 8.06 (d, 1H, ^3J = 9.3 Hz, JPt−H = 24.0 Hz), 8.40 (d, 1H, ^3J = 2.8 Hz, JPt−H = 4.3 Hz), 8.51 (ddd, 1H, ^3J = 7.7 Hz, ^3J = 7.7 Hz, ^4J = 1.6 Hz), 8.67 (d, 1H ^3J = 8.7 Hz), 9.07 (dd, 1H ^3J = 5.5 Hz, ^4J = 1.1 Hz, JPt−H = 7.3 Hz); ^{13}C{^{1}H} NMR (125 MHz, CD_2Cl_2): δ = −10.31 (^1JPt−C = 789.2, Pt−CH_3), 20.77, 40.5, 116.8 (JPt−C = 13.9 Hz), 120.3 (JPt−C = 39.8 Hz), 127.7 (JPt−C = 9.0 Hz), 128.8 (JPt−C = 117.5 Hz), 132.8 (JPt−C = 117.5 Hz), 142.7, 145.9, 146.6, 157.0 (JPt−C = 51.2 Hz), 160.94 (^1JPt−C = 1323.3 Hz, Pt−C_{car}); Anal. Calcd for $C_{16}H_{22}F_3N_3O_4PtS_2$: C, 30.19; H, 3.48; N, 6.60. Found: C, 30.35; H, 3.47; N, 6.62.

Substitution of Tetraphenylborate for Triflate. The triflate salts were dissolved in a small amount of methanol, and a concentrated solution of sodium tetraphenylborate (1 eq) was added dropwise, immediately precipitating the product. Cooling to −40 °C in the freezer and isolation on a glass frit gave >90% yield of the tetraphenylborate salts. A representative preparation is shown below.

[(5-(Dimethylamino)-*iso*-BIPY)Pt(CH_3)(DMSO)]$^+$ [BPh_4]$^-$ (4c). A few drops of DMSO were added to complex (**4b)** (0.400 g, 0.644 mmol) to dissolve it. After stirring the dark liquid under vacuum for 30 min. methanol (15 mL) was added. A solution of sodium tetraphenylborate (0.221 g, 0.644 mmol) in methanol (20, ml) was added dropwise with stirring to the orange solution. An orange precipitate formed upon addition. The mixture was filtered and the orange powder washed with diethyl ether and dried under vacuum. 0.467 g (yield = 90%). ^{1}H NMR (500 MHz, CD_2Cl_2) δ = 0.878 (s, 3H, ^2JPt−H = 80.32 Hz, Pt−CH_3), 3.03 (s, 6H, NMe_2), 3.26 (s, 6H, ^3JPt−H = 20.9 Hz, S(CH_3)$_2$), 6.86 (at, 4H, ^3J = 7.33 Hz), 7.02 (at, 8H, ^3J = 7.33 Hz), 7.35 (bs, 8H), 7.45 (d, 1H, ^3J = 8.64 Hz), 7.49 (dd, 1H, ^3J = 9.25 Hz, ^4J = 2.75 Hz), 7.63 (at, 1H, ^3J = 6.2 Hz), 7.73 (d, 1H, ^3J = 2.57 Hz), 7.99 (at, 1H, ^3J = 8.44 Hz), 8.03 (d, 1H, ^3J = 9.18 Hz), 9.90 (dd, 1H ^3J = 5.60 Hz, ^4J = 1.65 Hz); ^{13}C{^{1}H} NMR (125 MHz, CD_2Cl_2): δ = −11.12 (^1JPt−C = 788.8 Hz, Pt−CH_3), 39.96, 43.92, 114.6, 118.76 (JPt−C = 40.92 Hz), 122.0, 125.9, 127.2, 128.1 (JPt−C = 51.1 Hz), 133.3 (JPt−C = 110.0 Hz), 136.1, 142.5, 146.0, 146.2, 151.0, 156.0, 159.0, 164.2 (^1JB−C = 49.2 Hz); Anal. Calcd for $C_{39}H_{42}BN_3OPtS$: C, 58.06; H, 5.25; N, 5.21. Found: C, 57.79; H, 5.40; N, 5.11.

(4-(Dimethylamino)-*iso*-BIPY)Pt(CH_3)Br (3e). [(μ-SMe_2)Pt(CH_3)$_2$]$_2$ (0.6920 g, 1.20 mmol) was dissolved in 225 mL of methylene chloride to which was added *N*-(2-pyridyl)-4-(dimethylamino)-pyridinium bromide (0.6749 g, 2.41 mmol). Upon stirring the solution became yellow, and methane evolved. The reagents were left stirring for 8 h, and a crystalline yellow powder slowly precipitated from the solution. The volume was concentrated to 5 mL, and the solids isolated on a glass frit to give 0.660 g (56%) of **3e** as a bright yellow powder. Further concentration of the filtrate provided additional material. ^{1}H NMR (300 MHz, CD_3NO_2) δ = 0.91 (s, 3H, ^3JPt−H = 83.79 Hz, Pt−CH_3), 3.16 (s, 6H, N(CH_3)$_2$), 6.72 (dd, 1H, ^3J = 8.19 Hz, ^3J = 3.11 Hz), 7.04 (d, 1H, ^3JPt−H = 70.18 Hz ^3J = 3.27 Hz), 7.39 (m, 1H), 7.67 (d, 1H, ^3J = 8.96 Hz), 8.12 (m, 1H), 8.33 (d, 1H, ^3J = 8.04 Hz, ^3JPt−H = 6.42 Hz), 9.61 (dd, 1H ^3J = 5.51 Hz, ^4J = 1.60 Hz, ^3JPt−H = 6.63 Hz); Anal. Calcd for $C_{13}H_{16}BrN_3Pt$: C, 31.91; H, 3.30; N, 8.59. Found: C, 38.43; H, 4.49; N, 10.11.

[(4-(Dimethylamino)-*iso*-BIPY)Pt(CH_3)(DMSO)]$^+$ [BPh_4]$^-$ (3c). *N*-(2-pyridyl)-4-(dimethylamino)-pyridine-2-ylidene platinum methyl bromide (**3e**) (0.2400 g, 0.491 mmol), sodium tetraphenylborate (0.1679 g, 0.491 mmol) and dimethyl sulfoxide (105 μL, 1.484 mmol) were mixed with 250 mL of methylene chloride and left stirring overnight. In the morning the bright yellow solution had turned nearly colorless, and a white precipitate had formed. The mixture was filtered through Celite, and the volume concentrated to a total of 10 mL. Diethyl ether was slowly added to give a white precipitate. The suspension was placed in a −20°C freezer, and the white solids were isolated on a glass frit, washed with diethyl ether, and dried under high vacuum to give 0.365 g (92%) of **3c** as an off-white powder. ^{1}H NMR (300 MHz, CD_2Cl_2) δ = 0.70 (s, 3H, ^2JPt−H = 80.79 Hz Pt−CH_3), 3.09 (s, 3H, NCH_3), 3.21 (s, 3H, NCH_3), 3.21 (s, 6H, ^2JPt−H = 20.20 Hz Pt−S(CH_3)$_2$), 6.18 (dd, 1H, ^3J = 8.16 Hz, ^3J = 3.22 Hz), 6.83 (m, 5H), 6.94−7.04 (m, 9H), 7.33−7.47 (m, 10H), 7.90 (m, 1H), 9.61 (dd, 1H ^3J = 5.72 Hz, ^4J = 1.29 Hz, ^3JPt−H = 6.15 Hz); ^{13}C{^{1}H} (125 MHz, CD_2Cl_2): δ = −10.40 (^1JPt−C = 761.3 Hz, Pt−CH_3), 105.8, 110.4 (JPt−C = 118.79 Hz), 113.1, 123.7, 136.7, 141.7, 148.9, 153.8 (JPt−C = 60.5 Hz), 155.1, 163.6 (^1JPt−C = 1202.89 Hz, Pt−C_{car}). Anal. Calcd for $C_{39}H_{42}BN_3OPtS$: C, 58.06; H, 5.25; N, 5.21. Found: C, 57.79; H, 5.40; N, 5.11.

Synthesis of Carbonyl Cations 1d−4d. The dimethyl sulfide complexes **1b**−**4b** were dissolved in acetone (**1**,**2**,**4**) or prepared in situ (**3**) and degassed. Carbon monoxide (1 atm) was added and the solutions allowed to stir for 1 h. The carbonyl cations were precipitated by addition of diethyl ether and isolated on a glass frit. IR spectra were acquired in acetone. Anal. **2d** Calcd for $C_{17}H_{19}F_3N_2O_4PtS$: C, 34.06; H, 3.19; N, 4.67. Found: C, 33.73; H, 3.12; N, 4.40. **4d** Calcd for $C_{15}H_{16}F_3N_3O_4PtS$: C, 30.72; H, 2.75; N, 7.17. Found: C, 31.02; H, 2.73; N, 6.90.

($C_{11}H_8N$)Pt(CH_3)(DMSO) (6c). 2-Phenylpyridine (481 μL, 3.37 mmol) was added dropwise via syringe to a solution of [(μ-SMe_2)Pt-(CH_3)$_2$]$_2$ (0.967 g, 1.68 mmol) in 50 mL of acetone at room temperature in air. The solution quickly became yellow, and small bubbles formed. After stirring for 1.5 h DMSO (477 μL, 6.73 mmol) was added, and the solution stirred for another 30 min. The yellow solution was concentrated, and pentane was added, precipitating the bright yellow product. The suspension was filtered and dried under vacuum giving 0.864 g (58%) of **6c** as a bright yellow solid. ^{1}H NMR (300 MHz, acetone-d_6) δ = 0.66 (s, 3H, ^2JPt−H = 83.52 Hz, Pt−CH_3), 3.21 (s, 6H, ^2JPt−H = 17.6 Hz, S(CH_3)), 7.11 (dt, 1H, ^3J = 7.69 Hz, ^3J = 1.65 Hz), 7.21 (dt, 1H, ^3J = 7.74 Hz, ^3J = 1.65 Hz), 7.31−7.36 (m, 1H), 7.50 (d, 1H, ^3J = 1.1 Hz,^2JPt−H = 28.6 Hz), 7.34−7.79 (m, 1H), 8.03 (dd, 2H ^3J = 3.85 Hz, ^4J = 1.10 Hz) 9.80 (d, 1H ^3J = 5.60 Hz,^2JPt−H = 7.1 Hz); ^{13}C{^{1}H} (125 MHz, CD_2Cl_2): δ = −12.4 (^1JPt−C = 776.1, Pt−CH_3), 43.3 (JPt−C = 34.6), 118.4, 122.5, 123.3 (JPt−C = 39.3), 124.8, 129.0 (JPt−C = 66.7 Hz), 132.5 (JPt−C = 88.9 Hz), 137.9, 146.6, 150.3, 150.4 (JPt−C = 1062.8 Hz, Pt−C_{ph}), 164.0 (^1JPt−C = 74.9 Hz). Anal. Calcd for $C_{14}H_{17}NOPtS$: C, 38.01; H, 3.87; N, 3.17. Found: C, 38.12; H, 3.84; N, 3.15.

Acknowledgment. The authors would like to thank Lawrence M. Henling and Michael W. Day for assistance with X-ray crystallography and Ola F. Wendt for useful discussions. We gratefully acknowledge support from the MC^2 program in collaboration with bp.

Supporting Information Available: Erying plots and k_{obs} vs [DMSO] plots for **1c**−**4c** and **6** as well as relevant crystallographic data and pictures of structures for **1b**, **2c**−**4c**, **5**, and **6**. This material is available free of charge via the Internet at http://pubs.acs.org.

JA040075T